$\alpha(Z\alpha)^5 m$ finite-nuclear-size contribution to the energy levels in light muonic atoms

Savely G. Karshenboim*
Ludwig-Maximilians-Universität, Fakultät für Physik, 80799 München, Germany;
Max-Planck-Institut für Quantenoptik, Garching 85748, Germany;
and Pulkovo Observatory, St. Petersburg 196140, Russia

Evgeny Yu. Korzinin and Valery A. Shelyuto
D. I. Mendeleev Institute for Metrology, St. Petersburg 190005, Russia
and Pulkovo Observatory, St. Petersburg 196140, Russia

Vladimir G. Ivanov
Pulkovo Observatory, St. Petersburg 196140, Russia

(Received 16 August 2018; published 17 December 2018)

We present a theoretical consideration of the radiative two-photon finite-nuclear-size contributions to the Lamb shift in a light muonic atom. They are of the order of $\alpha(Z\alpha)^5 m$ and may depend differently on mR_N. The contributions are due to the electronic and muonic vacuum polarization and the muon self-energy. The consideration is done within the external field approximation. We also found the leading logarithmic finite-nuclear-size contributions in the next order. One of them is of the order $\alpha(Z\alpha)^6 \ln^2(Z\alpha)\,(mR_N)^2 m$ and the other is of the order $\alpha^2(Z\alpha)^5 \ln^2(m_e R_N)\,(mR_N)^3 m$. Special attention is paid to higher-order effects in muonic hydrogen and the related applications of various parametrizations of the proton electric form factors. We also consider the general expressions in coordinate space for the finite-size radiative contributions to the Lamb shift in two-body muonic atoms. The numerical results are present for the atoms with $Z \leqslant 10$.

DOI: 10.1103/PhysRevA.98.062512

I. INTRODUCTION

An accurate determination of the nuclear charge radii is an important problem of nuclear and atomic physics. Study of ordinary atoms allows us to determine the nuclear radii with an accuracy that is limited by the higher-order effects of quantum electrodynamics (QED) and atomic physics. An important exception is the study of the isotopic shift, the theory of which provides us with massive cancelations of various higher-order contributions.

There is another opportunity within atomic physics to reach high accuracy in the value of the nuclear charge radius, namely the study of muonic atoms. Our interest in this paper is with the Lamb shift in two-body muonic atomic systems (muon-nucleus). In such a case, the nuclear effects are enhanced and the required QED theory is essentially simpler than in the case of the ordinary atoms (where a more accurate theory is required for the same accuracy in the value of the radius). The atomic part of the calculations is also (relatively) simple as far as it concerns two-body atoms.

Still there is an additional problem there due to higher-order nuclear-structure contributions. In muonic atoms they serve as the limiting factor for the accuracy in the determination of the nuclear radius. In this paper, we study higher-order finite-nuclear-size (FNS) contributions. (There are also nuclear polarizability contributions, which are beyond the consideration of our paper.)

The leading FNS contribution for the nl state in a hydrogenlike atom is of the form

$$\Delta E_{\rm fns:lead}(nl) = \frac{2}{3}\frac{(Z\alpha)^4 m_r}{n^3}\,(m_r R_N)^2\,\delta_{l0}, \qquad (1)$$

where Z is the nuclear charge and R_N is the rms nuclear charge radius; m is the mass of the orbiting particle, which is a muon in our paper (except for the case when we explicitly discuss "ordinary" atoms with $m = m_e$);

$$m_r = \frac{mM}{M+m}$$

is the reduced mass of the two-body problem and M is the nuclear mass. The relativistic units in which $\hbar = c = 1$ are applied throughout the paper.

The leading terms in (1) may be interpreted in two ways. One may compare theory and experiment, and in this case a numerical value of the leading FNS term must be obtained. The other option is a determination of the nuclear radius. In such a case for all the terms (with a few exceptions to be discussed below) but the leading FNS term, the numerical values should be obtained, while the leading FNS term should remain in the form

$$\Delta E_{\rm fns:lead}(ns) = \frac{8}{n^3}\,C_{\rm lead:fns}\,\frac{R_N^2}{\rm fm^2}, \qquad (2)$$

*savely.karshenboim@mpq.mpg.de

TABLE I. The leading FNS contribution to the Lamb shift of the ns states in light muonic atoms [following (2)] and the atomic parameters relevant for its calculation. The masses are taken from [1] for $A \leqslant 4$ and from [2] for heavier elements. As for the radii, we used the following sources: [3] for the proton, [4] for the other $Z = 1$ nuclei, [5] for $Z = 2$, and [6] for $Z > 2$.

Nucleus	Z	M (u)	R_N (fm)	$C_{\text{lead:fns}}$ (meV)	$E_{\text{lead:fns}}(2s)$ (meV)
^{1}H	1	1.007 276	0.879(11)	5.1974	4.02(10)
^{2}H	1	2.013 553	2.130(10)	6.0732	27.55(26)
^{3}H	1	3.015 501	1.755(87)	6.4078	19.7(20)
^{3}He	2	3.014 932	1.973(16)	102.52	399.1(65)
^{4}He	2	4.001 506	1.681(4)	105.32	298(14)
^{6}Li	3	6.013 477	2.589(39)	548.22	$367(11) \times 10$
^{7}Li	3	7.014 358	2.444(42)	552.59	$330(11) \times 10$
^{9}Be	4	9.009 989	2.519(12)	1765.1	$1120(11) \times 10$
^{10}B	5	10.010 19	2.428(50)	4325.3	$255(11) \times 10^2$
^{11}B	5	11.006 56	2.406(29)	4338.5	$251.1(6.1) \times 10^2$
^{12}C	6	11.996 71	2.4702(22)	9019.1	$550.3(1.0) \times 10^2$
^{13}C	6	13.000 06	2.4614(34)	9038.7	$547.6(1.5) \times 10^2$
^{14}N	7	13.999 23	2.5582(70)	16 776	$109.79(0.6) \times 10^3$
^{15}N	7	14.996 27	2.6058(80)	16 803	$114.10(0.7) \times 10^3$
^{16}O	8	15.990 53	2.6991(52)	28 706	$209.13(81) \times 10^3$
^{17}O	8	16.994 74	2.6932(75)	28 742	$208.5(1.2) \times 10^3$
^{18}O	8	17.994 77	2.7726(56)	28 773	$221.19(89) \times 10^3$
^{19}F	9	18.993 47	2.8976(25)	46 135	$387.35(67) \times 10^3$
^{20}Ne	10	19.986 95	3.0055(21)	70 379	$635.74(89) \times 10^3$
^{21}Ne	10	20.988 36	2.9695(33)	70 436	$621.1(1.4) \times 10^3$
^{22}Ne	10	21.985 90	2.9525(40)	70 488	$614.5(1.7) \times 10^3$

where we normalized the coefficient $C_{\text{lead:fns}}$ to the coefficient for the $2s$ state. The numerical values for the interpretations of the leading FNS contribution for the light muonic atoms are summarized in Table I for the relevant nuclear parameters.

In this paper, we consider some higher-order FNS terms. Those terms depend on the value of the nuclear charge radius and can also be an exception from the numerical calculation while determining the nuclear radius.

The higher-order effects mostly affect the ns states, and we focus on the related theory. The total FNS result can be presented as

$$\Delta E_{\text{fns:total}}(ns) = \mathcal{F}(Z\alpha, Z\alpha m_r R_N)\, \Delta E_{\text{fns:lead}}(ns). \qquad (3)$$

There are also other parameters such as α for radiative corrections (which is presented as an overall factor for some contributions) and m/M for the recoil effects, but those two, $Z\alpha$ and $Z\alpha m_r R_N$, mentioned above explicitly, are the most important as dynamic parameters, which characterize the relation between the involved characteristic distances and/or momenta.

In atomic physics with ordinary atoms, we should consider a situation when

$$(Z\alpha)^2 \gg Z\alpha m R_N.$$

In other words, we are mostly interested in relativistic corrections [= expansion in $(Z\alpha)$] to the leading FNS term, rather than in higher-order finite-size effects due to the expansion in $Z\alpha m R_N$. In muonic atoms, mR_N is about unity (in the lightest of them) and essentially above unity in the heavy ones, which makes the expansion in $Z\alpha m R_N$ more important than the relativistic corrections to the leading FNS term. The physical meaning of those two expansions is very different. The relativistic corrections depend on the details of the shape of the charge distribution relatively weakly, while the expansion in $Z\alpha m R_N$ directly deals with higher momenta of the distribution.

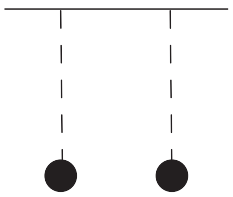

FIG. 1. The Friar contribution in order $(Z\alpha)^5(mR_N)^3m$. The appropriate subtractions are assumed (see the explanation in Sec. II). The closed circles are for the extended nucleus.

The most important FNS contributions are studied within the external field approximation (i.e., with a zero energy transfer $q_0 = 0$ through each photon line). In principle, some FNS recoil contributions have also been studied (see, e.g., [7–14]). However, they are smaller than the external-field corrections to the leading term (1) and are not a concern of this paper.

The next-to-leading FNS contribution in the external field approximation is of order $Z\alpha m R_N$ with respect to the leading FNS term in (1). Table I allows us to estimate not only the leading FNS term, but also the value of the expansion parameter $Z\alpha m R_N$. The values of the nuclear radius are given there in fermis, and we note that $m_\mu \times 1\ \text{fm} \simeq 0.535$.

The correction in order $(Z\alpha)^5(mR_N)^3m$ is called the Friar term (see Fig. 1). Most of our paper is devoted to a consideration of radiative FNS corrections in order $\alpha(Z\alpha)^5m$. Their dependence on mR_N is somewhat different for different contributions. Those contributions are two-photon exchange contributions, as is the Friar term, and technically they are corrections to the Friar term rather than to the leading FNS term in (1).

II. THE FRIAR TERM [OF ORDER $(Z\alpha)^5(mR_N)^3m$] AND RADIATIVE CORRECTIONS TO IT

While in ordinary atoms the most important higher-order FNS correction is due to the relativistic effects, in the case of light muonic atoms the most important higher-order FNS contribution is the Friar term (see Fig. 1), which is of order $(Z\alpha)^5(mR_N)^3m$. In contrast to the leading term, it cannot be expressed in terms of a certain low-q property, such as a certain (standard) moment of the charge distribution.

The consideration of the Friar term can be done in both coordinate space [15,16],

$$\Delta E_{\text{fns:Fr}}(ns) = -\frac{(Z\alpha)^5\, m_r^4}{3n^3} \int d^3r\, d^3r'\, \hat{\rho}_E(\mathbf{r})\hat{\rho}_E(\mathbf{r}')|\mathbf{r}-\mathbf{r}'|^3, \qquad (4)$$

or momentum space [17,18],

$$\Delta E_{\rm fns:Fr}(ns) = -\frac{16(Z\alpha)^5\, m_r^4}{\pi n^3} \int_0^\infty \frac{dq}{q^4} \times [[G_E(q^2)]^2 - 1 - 2G'_E(0)\, q^2], \quad (5)$$

where $G_E(q^2)$ is the electric form factor and q^2 is the Euclidian momentum. Most of the applications in this paper relate to the external field approximation, where $q^2 = \mathbf{q}^2$. The value $\hat\rho_E(\mathbf{r})$ relates to the charge distribution (see below for an accurate definition).

The diagrams for the Friar term (see Fig. 1) have certain subtractions. Those subtractions are generated *ab initio* while transforming the "complete" expressions (see [18] for details). One of them is due to a need to subtract a pointlike part from the full vertex of the "extended" nucleus [such as "-1" in the numerator

$$[G_E(q^2)]^2 - 1 - 2G'_E(0)\, q^2$$

in (5)], while the other [such as the $G'(0)$ term there] is due to a rearrangement of the diagrams in order to separate $(Z\alpha)^4$ and $(Z\alpha)^5$ contributions [cf. (1) and (5)].

From the point of view of the definition, the Friar term could be defined as proportional to $m m_r^3$ and m_r^4. We use the latter throughout the paper.

Both of those definitions are applicable and are used in the literature. The difference in the definitions means neither a discrepancy nor an ambiguity. That is a question what should be referred to as the "recoil" contributions. Only the sum of the "nonrecoil" Friar term and the two-photon "recoil" FNS correction has meaning.

The result for the contribution is expressed in terms of a specific convolution in coordinate space,

$$\Delta E_{\rm fns:Fr}(ns) = -\frac{(Z\alpha)^5\, m_r^4}{3n^3}\, \langle r^3\rangle_{(2)},$$
$$\langle r^3\rangle_{(2)} \equiv \int d^3r\, d^3r'\, \hat\rho_E(\mathbf{r})\hat\rho_E(\mathbf{r}')|\mathbf{r}-\mathbf{r}'|^3 = \frac{48}{\pi}\int_0^\infty \frac{dq}{q^4}[[G_E(q^2)]^2 - 1 - 2G'_E(0)\, q^2], \quad (6)$$

which is referred to as the Friar moment, or the third Zemach moment.

The electric form factor of the nucleus $G_E(\mathbf{q}^2)$ is a directly measurable function, while its Fourier transform

$$\hat\rho_E(\mathbf{r}) = \frac{1}{(2\pi)^3}\int d^3\mathbf{q}\, e^{i\mathbf{r}\cdot\mathbf{q}}\, G_E(\mathbf{q}^2)$$

does not have any simple physical meaning. [We use the notation $\hat\rho_E(\mathbf{r})$ to distinguish it from the "true" charge density distribution $\rho_E(\mathbf{r})$.] Sometimes $\hat\rho_E(\mathbf{r})$ is referred to as the charge distribution in the Breit frame. We have to remember that such a frame exists only for the fixed initial and final momenta of the scattered nucleus, i.e., it is well defined in momentum space. The evaluation of the Fourier transformation in (6) involves different momenta and therefore different "Breit frames."

Taking into account the difference between $\hat\rho_E(\mathbf{r})$ and $\rho_E(\mathbf{r})$ and the measurability of the form factor $G_E(\mathbf{q}^2)$, the rms nuclear charge radius is defined not as

$$\int d^3r\, \rho_E(\mathbf{r})\mathbf{r}^2, \quad (7)$$

but as

$$R_N^2 \equiv -6\,\frac{\partial G(q^2)}{\partial q^2}\bigg|_{q^2=0}. \quad (8)$$

The terminology is somewhat confusing. Equation (8) is the exact *definition* of the rms charge radius, which is used in all *ab initio* calculations, while Eq. (7) is an approximate presentation of that radius (assuming the nonrecoil approximation).

In the case of nuclei (even the light ones), the most important area of the charge distribution is essentially larger than the Compton wavelength of the nucleus. That means that outside of a central area with $r \sim 1/m_N$, the Fourier transform $\hat\rho_E(\mathbf{r})$ is close to the density of the charge distribution $\rho_E(\mathbf{r})$. The difference between these two concepts is due to the nuclear recoil (while absorbing or emitting a photon), so in the "nonrecoil" limit those two functions, $\rho_E(\mathbf{r})$ and $\hat\rho_E(\mathbf{r})$, coincide.

The difference between two definitions above [see (7) and (8)] is due to recoil effects, which have been calculated occasionally only for definition (8). Those two definitions are slightly different but equally applicable to the atomic systems, where the recoil effects have not been studied or can be neglected. That is correct in general (for an atomic system), but it can be also applied to a particular order of magnitude, say, to $\alpha(Z\alpha)^5 m$.

Nowadays, for muonic hydrogen most of the evaluations of the Friar term are performed in momentum space. Calculations are not free of problems. Some of them are discussed for muonic hydrogen in [13,19] (cf. [20]).

Calculations in coordinate space have been performed for some light muonic atoms (see, e.g., [21–28]) other than muonic hydrogen. The result comes from the nuclear-physics models. We do not discuss here the accuracy of such an evaluation, which is hard to estimate directly. The coordinate-space evaluation is always model-dependent. (Use of the chiral perturbative theory to build an effective nucleon-nucleon interaction [29–36], which is a breakthrough in this area, reduces such a model dependence, but does not eliminate it.)

Since the accuracy of the Friar term is improving, it is important to consider corrections to it, such as a radiative FNS correction of order $\alpha(Z\alpha)^5 m$, and to find out how they depend on the parameter $m R_N$. There are three types of radiative FNS corrections. They can be caused by the electron vacuum polarization (eVP), by the vacuum polarization (VP) of muons, and by the self-energy (SE) of the muon. The latter two are similar to the related FNS corrections in electronic hydrogenlike atoms (VP for the same type of particles as the orbiting one and SE). They can be present in terms of "hard" two-photon exchange contributions where the momentum transfer is of the same order as the mass of the orbiting particle m or as the inverse nuclear charge radius R_N^{-1}. All those hard FNS corrections have order $\alpha(Z\alpha)^5 m$.

On the contrary, the eVP contribution in muonic atoms is a specific one for those atoms. The relation $m_e \sim \alpha m_\mu$ leads to effective potentials with the radius comparable to the Bohr radius of the atoms. The eVP contributions may be both "soft"

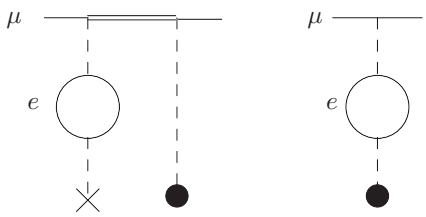

FIG. 2. The Uehling-potential (eVP) correction to FNS contribution in order $\alpha(Z\alpha)^4 m$. The double horizontal line is for the Coulomb Green function of the muon.

and "hard" depending on the structure of the diagram. In soft contributions, the momentum transfer is characterized by the atomic momentum, while in the hard part the momentum transfer through the VP loop is about m or R_N^{-1} and therefore larger than m_e. The soft radiative FNS corrections appear in the orders $\alpha(Z\alpha)^4 m$ and $\alpha(Z\alpha)^5 m$. The hard eVP FNS contribution is of order $\alpha(Z\alpha)^5 m$.

The eVP FNS corrections of order $\alpha(Z\alpha)^4 m$ have been studied for a while [17,18,37–39]. In this paper, we focus on the $\alpha(Z\alpha)^5 m$ FNS contributions, but first we provide a brief overview of the $\alpha(Z\alpha)^4 m$ terms.

III. CONTRIBUTION OF THE ELECTRON VACUUM POLARIZATION

Let us recall the evaluation of the leading FNS term of order $(Z\alpha)^4 m$ in (1) and of the leading radiative correction to it [of order $\alpha(Z\alpha)^4 m$]. The Coulomb interaction of a pointlike nucleus reads

$$-\frac{4\pi Z\alpha}{q^2},$$

while for the extended one it takes the form

$$-\frac{4\pi Z\alpha}{q^2}G(q^2) = -\frac{4\pi Z\alpha}{q^2} - 4\pi Z\alpha\frac{\partial G(q^2)}{\partial q^2} + \cdots, \qquad (9)$$

where the first term is the pointlike contribution while the second one is proportional to $R_N^2\delta(\mathbf{r})$ (in coordinate space). The latter produces the leading FNS term (1),

$$-4\pi Z\alpha\left(-\frac{R_N^2}{6}\right)\langle\delta(\mathbf{r})\rangle = \frac{2}{3}\pi\,(Z\alpha)\,R_N^2\,|\psi_{nl}(0)|^2, \qquad (10)$$

where the value of the (nonrelativistic) wave function at the origin for the nl state is

$$|\psi_{nl}(0)|^2 = \frac{(Z\alpha)^3 m^3}{\pi}\frac{\delta_{l0}}{n^3}. \qquad (11)$$

One can see that the result for the leading FNS term is a matrix element over the correction to the Coulomb field due to the finite size of the nucleus. Let us consider now the Uehling correction to the leading FNS term, which is the eVP correction (see Fig. 2). We should consider two types of contributions. One is due to the Uehling correction to the electrostatic field of the extended nucleus, i.e., to the δ function, and the other is due to a correction to the wave function at the origin.

The complete result for the eVP FNS correction in order $\alpha(Z\alpha)^4 m$, which is the leading radiative FNS contribution, reads

$$\Delta E_{\text{fns:eVP:lead}}(nl) = \frac{\alpha}{\pi}C_1(nl)\,\Delta E_{\text{fns:lead}}(ns), \qquad (12)$$

where

$$C_1(nl) = C_1^{(\psi)}(n) + C_1^{\text{FNS}}(nl),$$

with $C_1^{(\psi)}(nl)$ being the correction due to the wave function,

$$|\psi_{ns}(0)|^2 \to \left(1 + \frac{\alpha}{\pi}C_1^{(\psi)}(ns)\right)|\psi_{ns}(0)|^2. \qquad (13)$$

That is a "generic" part of the eVP corrections to any contribution, which is proportional to $|\psi_{ns}(0)|^2$. It is known in a semianalytic form [40–43]

$$C_1^{(\psi)}(1s) = \frac{\pi(\kappa^2-2)}{2\kappa^3} + \frac{6-8\kappa^2+5\kappa^4}{3\kappa^2(1-\kappa^2)} + \frac{2-4\kappa^2+3\kappa^4-2\kappa^6}{\kappa^3(1-\kappa^2)}\mathcal{A}(\kappa) + J(\kappa),$$

$$C_1^{(\psi)}(2s) = \frac{\pi\left(3\kappa_2^2-26\right)}{3\kappa_2^3} + \frac{312-920\kappa_2^2+894\kappa_2^4-195\kappa_2^6+44\kappa_2^8}{18\kappa_2^2\left(1-\kappa_2^2\right)^3}$$

$$+\frac{104-376\kappa_2^2+506\kappa_2^4-309\kappa_2^6+42\kappa_2^8-12\kappa_2^{10}}{6\kappa_2^3\left(1-\kappa_2^2\right)^3}\mathcal{A}(\kappa_2) + L(\kappa_2), \qquad (14)$$

where

$$\kappa_n = \frac{\kappa}{n} = \frac{Z\alpha m_r}{m_e\,n},$$

$$\mathcal{A}(z) = \begin{cases} \frac{\arccos z}{\sqrt{1-z^2}}, & z<1, \\ \frac{\ln(z+\sqrt{z^2-1})}{\sqrt{z^2-1}}, & z>1, \end{cases}$$

and

$$J(z) = -\frac{2z^2}{3}\int_0^1 \frac{y\sqrt{1-y^2}(y^2+2)}{(1+yz)^2}\ln\frac{yz}{1+yz},$$

$$L(z) = -\frac{4z^2}{3}\int_0^1 \frac{y\sqrt{1-y^2}(y^2+2)(y^2z^2+2)}{(1+yz)^4}\ln\frac{yz}{1+yz}.$$

TABLE II. The numerical results for the wave-function correction for the $1s$ and $2s$ states in light muonic atoms ($Z \leqslant 10$) (cf. [41,43]) following (14).

Nucleus	κ	Z	$C_1^{(\psi)}(1s)$	$C_1^{(\psi)}(2s)$
^{1}H	1.3562	1	1.7312	1.4043
^{2}H	1.4284	1	1.8012	1.4523
^{3}H	1.4542	1	1.8256	1.4690
^{3}He	2.9083	2	2.9050	2.1818
^{4}He	2.9345	2	2.9204	2.1920
^{6}Li	4.4428	3	3.6599	2.6942
^{7}Li	4.4546	3	3.6648	2.6976
^{8}Be	5.9511	4	4.2067	3.0926
^{9}Be	5.9604	4	4.2097	3.0949
^{10}B	7.4598	5	4.6392	3.4278
^{11}B	7.4674	5	4.6412	3.4294
^{12}C	8.9684	6	4.9963	3.7181
^{13}C	8.9749	6	4.9977	3.7193
^{14}N	10.4771	7	5.3001	3.9742
^{15}N	10.4827	7	5.3012	3.9751
^{16}O	11.9859	8	5.5644	4.2033
^{17}O	11.9909	8	5.5652	4.2040
^{18}O	11.9953	8	5.5659	4.2046
^{19}F	13.4991	9	5.7987	4.4109
^{20}Ne	15.0035	10	6.0076	4.5991
^{21}Ne	15.0075	10	6.0081	4.5996
^{22}Ne	15.0112	10	6.0086	4.6000

TABLE III. The eVP FNS contribution of order $\alpha(Z\alpha)^4 m$ to the Lamb shift of the lower levels in light muonic atoms ($Z \leqslant 10$). C_1 is defined in (12).

Nucleus	Z	$C_1(1s)$	$C_1(2s)$	$C_1(2p)$	$C_1(2p-2s)$
^{1}H	1	2.6142	2.3145	–0.01745	–2.3320
^{2}H	1	2.7116	2.3909	–0.01840	–2.4093
^{3}H	1	2.7457	2.4175	–0.01873	–2.4362
^{3}He	2	4.2250	3.5390	–0.03259	–3.5716
^{4}He	2	4.2459	3.5548	–0.03277	–3.5875
^{6}Li	3	5.2448	4.3185	–0.04041	–4.3589
^{7}Li	3	5.2514	4.3236	–0.04045	–4.3641
^{8}Be	4	5.9796	4.9053	–0.04480	–4.9501
^{9}Be	4	5.9836	4.9085	–0.04482	–4.9533
^{10}B	5	6.5592	5.3875	–0.04753	–5.4351
^{11}B	5	6.5618	5.3898	–0.04754	–5.4373
^{12}C	6	7.0370	5.7984	–0.04934	–5.8477
^{13}C	6	7.0389	5.8000	–0.04935	–5.8494
^{14}N	7	7.4433	6.1567	–0.05060	–6.2073
^{15}N	7	7.4447	6.1580	–0.05061	–6.2086
^{16}O	8	7.7964	6.4745	–0.05152	–6.5260
^{17}O	8	7.7975	6.4755	–0.05152	–6.5270
^{18}O	8	7.7984	6.4763	–0.05152	–6.5279
^{19}F	9	8.1094	6.7606	–0.05220	–6.8128
^{20}Ne	10	8.3883	7.0187	–0.05272	–7.0714
^{21}Ne	10	8.3890	7.0193	–0.05272	–7.0720
^{22}Ne	10	8.3896	7.0199	–0.05272	–7.0726

We summarize the numerical results on the correction to the wave function at the origin for the $1s$ and $2s$ states in Table II.

In contrast to the correction to the wave function, the correction due to the modification of the contact term is specific for any contact term. In the case of the FNS contributions in order $\alpha(Z\alpha)^4 m$ [40] (cf. [17,41,44] and [45–47]), the result is of the form

$$
\begin{aligned}
C_1^{\rm FNS}(1s) &= -\frac{\pi}{3\kappa^3} + \frac{6+\kappa^2}{9\kappa^2} + \frac{2-\kappa^2+2\kappa^4}{3\kappa^3}\mathcal{A}(\kappa),\\
C_1^{\rm FNS}(2s) &= -\frac{\pi}{3\kappa_2^3} + \frac{24-44\kappa_2^2-29\kappa_2^4+22\kappa_2^6}{36\kappa_2^2\left(1-\kappa_2^2\right)^2}\\
&\quad + \frac{8-20\kappa_2^2+33\kappa_2^4-20\kappa_2^6+8\kappa_2^8}{12\kappa_2^3\left(1-\kappa_2^2\right)^2}\mathcal{A}(\kappa_2),\\
C_1^{\rm FNS}(2p) &= -\frac{\pi}{3\kappa_2^3} + \frac{24-44\kappa_2^2+13\kappa_2^4-2\kappa_2^6}{36\kappa_2^2\left(1-\kappa_2^2\right)^2}\\
&\quad + \frac{8-20\kappa_2^2+15\kappa_2^4}{12\kappa_2^3\left(1-\kappa_2^2\right)^2}\mathcal{A}(\kappa_2). \qquad (15)
\end{aligned}
$$

The complete result for the eVP FNS contributions for low states is tabulated in Table III.

The corrections have been considered often in literature, where the details of the calculations can be found. In particular, in the case of muonic hydrogen, the eVP correction to the proton-finite-size contribution for the s states has been known for a while [17,18,37–39], basically numerically [48]. Some technical details can be found in [40–43] (where the eVP correction to the wave function at the origin required for calculation of the left diagram in Fig. 2 was studied), in [40] (where the result for the right graph in Fig. 2 was obtained in closed analytic form), and in [17,41,44] [where a closely related contribution to the HFS in muonic hydrogen (the eVP correction) was calculated].

As we already mentioned, many FNS contributions are of the same generic form [cf. (10)], being expressed in terms of a matrix element over a contact term and therefore being proportional to $|\psi(0)|^2$. For instance, the Friar term in (5) is of such a form. The Uehling corrections to them, to the leading FNS term, and to the Friar term are also of a similar form. There is a Uehling correction to $|\psi(0)|^2$ and there is a correction to the contact term (see above for the Uehling correction to the leading FNS term). The correction to $|\psi_{ns}(0)|^2$ is a universal one (see Fig. 3), while the correction to the contact term depends on the phenomena we consider.

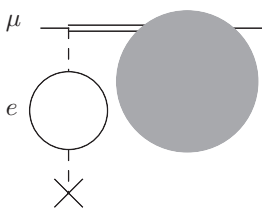

FIG. 3. The Uehling (eVP) correction to the calculation of the contact matrix element (the big closed circle) over the wave functions at the origin, i.e., due to the eVP correction to $|\psi(0)|^2$.

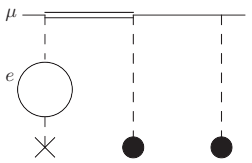

FIG. 4. The soft eVP FNS contribution (eVP:soft) due to the Uehling correction to the perturbed wave functions.

The mentioned generic Uehling correction to the Friar term (see Fig. 4) is of the form [cf. (13)]

$$\Delta E_{\rm fns:eVP:soft}(ns) = \frac{\alpha}{\pi}\, C_1^{(\psi)}(ns)\, \Delta E_{\rm fns:Fr}(ns). \tag{16}$$

For $l \neq 0$ the correction vanishes.

That is a "soft" contribution in a sense that the characteristic momentum transfer through the eVP loop is $Z\alpha m_\mu$. Still with an increase of the nuclear charge Z we may consider a limit $Z\alpha m_\mu \gg m_e$, which leads to the asymptotic behavior (cf., e.g., [39–41,43])

$$\Delta E_{\rm fns:eVP:soft}(ns) \simeq 3 \times \frac{2}{3}\,\frac{\alpha}{\pi}\,\ln\frac{Z\alpha m_\mu}{m_e}\,\Delta E_{\rm fns:Fr}(ns). \tag{17}$$

As we mentioned above, there is also a "hard" eVP contribution to the Friar term that is a specific term for muonic atoms. In ordinary atoms, the orbiting particle is an electron and the VP loop is an eVP one, which means that the orbiting particle and the particle in the closed loop are of the same type. The related diagram in muonic atoms is the one where both the orbiting particle and the particle in the closed loop are muons. It is considered in Sec. IV, while here we consider a specific contribution where the loop's particle is essentially lighter than the orbiting one.

To calculate the hard part of the eVP correction to the Friar contribution, one has to insert the eVP factor into the integrand of the Friar term in (5). Taking into account the combinatoric factor of 2, we arrive at

$$\Delta E_{\rm eVP:hard}(ns) = -\frac{32\alpha(Z\alpha)^5}{\pi^2 n^3}\, m_r^4 \int \frac{dq}{q^2}\, I_e(q^2) \times [[G_E(q^2)]^2 - 1 - 2G'_E(0)\, q^2], \tag{18}$$

where

$$I_e(q^2) = \int_0^1 dv \frac{v^2(1-v^2/3)}{4m_e^2 + (1-v^2)q^2}. \tag{19}$$

The characteristic momentum transfer in the Friar contribution (see Sec. II) is $R_N^{-1} \gg m_e$ and therefore we may apply the asymptotic formula for the eVP insertion

$$I_e(q^2) \to I_e^{\rm as}(q^2) = \frac{1}{q^2}\left(\frac{1}{3}\ln\frac{q^2}{m_e^2} - \frac{5}{9}\right). \tag{20}$$

That leads to the expression for the "hard" part of the eVP contribution (see Fig. 5) in momentum space as

$$\Delta E_{\rm fns:eVP:hard}(ns) = -\frac{32\,\alpha(Z\alpha)^5\, m_r^4}{\pi^2 n^3} \times \int_0^\infty \frac{dq}{q^4}\left(\frac{1}{3}\ln\frac{q^2}{m_e^2} - \frac{5}{9}\right) \times [[G_E(q^2)]^2 - 1 - 2G'_E(0)\, q^2]. \tag{21}$$

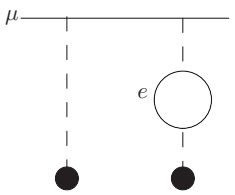

FIG. 5. Specific-muonic-atom FNS contribution in order $\alpha(Z\alpha)^5 m$: a hard one-loop electron-vacuum-polarization contribution (eVP:hard). The necessary subtraction is assumed.

In coordinate space, the result takes the form

$$\Delta E_{\rm fns:eVP:hard}(ns) = -\frac{2\alpha(Z\alpha)^5\, m_r^4}{3\pi n^3} \times \left\langle r^3\left[\frac{2}{3}\left(\ln\frac{1}{m_e r} + C''\right) - \frac{5}{9}\right]\right\rangle_{(2)}, \tag{22}$$

where the constant is

$$C'' = \frac{25}{12} - \gamma = 1.506\,12\ldots,$$

and $\gamma \simeq 0.577\,216\ldots$ is Euler's constant.

It may be useful to present the logarithmic term as

$$\left\langle r^3 \ln\frac{1}{m_e r}\right\rangle_{(2)} = \left\langle r^3\left(\ln\frac{1}{m_e R_N} + \ln\frac{R_N}{r}\right)\right\rangle_{(2)},$$

and to evaluate the second term for some particular charge distributions.

For the homogeneous-sphere distribution, the result is

$$\left\langle r^3 \ln\frac{R_N}{r}\right\rangle_{(2)} = \left(\frac{53}{126} - \frac{1}{2}\ln\frac{20}{3}\right)\langle r^3\rangle_{(2)} \simeq -0.527\,925\ldots\,\langle r^3\rangle_{(2)}. \tag{23}$$

Altogether, we find for the homogeneous-sphere distribution

$$\Delta E_{\rm fns:eVP:hard}(ns) \simeq \frac{\alpha}{\pi}\left(\frac{4}{3}\ln\frac{1}{m_e R_N} - \frac{2}{3}\ln\frac{20}{3} - \frac{4}{3}\gamma + \frac{421}{189}\right)\Delta E_{\rm fns:Fr}(ns), \tag{24}$$

which could be applied for various estimations for light muonic atoms, but not for muonic hydrogen.

The related relation for the dipole parametrization, which is more appropriate for rough estimations for muonic hydrogen, reads

$$\left\langle r^3 \ln\frac{R_N}{r}\right\rangle_{(2)} = \left(-\frac{3197}{1260} + \gamma + \frac{1}{2}\ln 12\right)\langle r^3\rangle_{(2)} \simeq -0.717\,633\ldots\,\langle r^3\rangle_{(2)} \tag{25}$$

and

$$\Delta E_{\rm fns:eVP:hard}(ns) \simeq \frac{\alpha}{\pi}\left(\frac{4}{3}\ln\frac{1}{m_e R_N} + \frac{2}{3}\ln 12 - \frac{1622}{945}\right)\Delta E_{\rm fns:Fr}(ns). \tag{26}$$

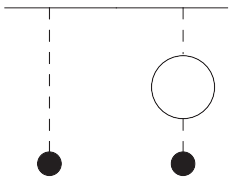

FIG. 6. Hard FNS contribution in order $\alpha(Z\alpha)^5 m$: one-loop vacuum-polarization contribution. The necessary subtraction is assumed. In ordinary atoms, the orbiting particle is an electron and the VP loop is an eVP one, while in a muonic atom both the orbiting particle and the particle in the closed loop are muons. The case of eVO contributions in muonic atoms is considered separately (see Fig. 5 in Sec. III).

The leading asymptotic term, enhanced by a large logarithm, in (24) and (26) is obviously the same and can be easily found applying the logarithmic approximation to (22). It is

$$\Delta E_{\text{fns:eVP:hard}}(ns) \simeq 2 \times \frac{2}{3}\frac{\alpha}{\pi} \ln\frac{1}{m_e R_N}\, \Delta E_{\text{fns:Fr}}(ns). \quad (27)$$

Using the logarithmic approximation, one can also find a double-logarithmic correction in the next order in α,

$$\Delta E_{\text{fns:eVP:2}}(ns) \simeq 3 \times \frac{4\alpha^2}{9\pi^2} \ln^2(m_e R_N)\, \Delta E_{\text{fns:Fr}}(ns), \quad (28)$$

which is small.

IV. CONTRIBUTION OF THE MUON VACUUM POLARIZATION

A calculation of a FNS contribution always involves some subtractions. The "minimal" case is when one subtracts from the extended nucleus its pointlike limit. A more sophisticated case is when it is necessary to subtract also the contributions of the "lower" order. In the case of the leading FNS term in (1) one has to deal with the first scenario. The leading term is the contribution of the lowest order possible. Meanwhile, the Friar term [see (5)] is a correction that is of a higher order than the leading term. It involves two subtractions that are clearly seen in the integrand in momentum space in (5). $G[(q^2)]^2$ is due to the extended nucleus, the subtraction of unity obviously relates to the pointlike physics [$G(q^2) \to 1$], while the third term with $G'(0)$ is due to the subtraction of the lower-order contribution, i.e., the leading FNS term (1), which is proportional to the rms charge radius as defined in (8).

The Friar term is presented above as a hard two-photon-exchange contribution [see (5)]. The structures related to the lower orders manifest themselves as infrared divergent terms in the hard limit, when the atomic momentum and energies are neglected inside the diagram. Therefore, after the removal of such structures by the appropriate subtractions, the related diagrams become infrared-finite.

As we mentioned, there are radiative FNS corrections of order $\alpha(Z\alpha)^5 m$ due to muonic vacuum polarization and the muon's self-energy (see Figs. 6 and 7). In ordinary atoms, one can also consider similar contributions (see, e.g., [18]). In the case of the VP contribution, the particle in the VP loop should be of the same kind as the orbiting one, i.e., an electron in ordinary atoms.

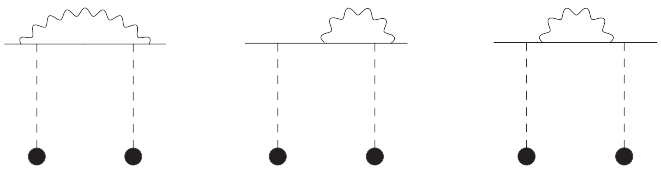

FIG. 7. Hard FNS contributions in order $\alpha(Z\alpha)^5 m$: one-loop self-energy contribution. The necessary subtraction is assumed.

The closed circles in the diagrams are for the nuclear vertex with the electric form factor $G_E(q^2)$, and the subtraction of the pointlike contributions

$$[G_E(q^2)]^2 - 1 \quad (29)$$

is assumed. Since the radiative corrections soften the q-integral at low q, there is no FNS contribution in order $\alpha(Z\alpha)^4 m$, and for the two-photon diagrams in Figs. 6 and 7 only one subtraction is required.

Due to the difference in the subtractions, the structure of the expression for the (μ)VP FNS contribution in order $\alpha(Z\alpha)^5 m$ differs from that for the eVP one [cf. (18)]. Following [18], for example, we find for the VP FNS contribution

$$\Delta E_{\text{fns:VP}}(ns) = -\frac{32\alpha(Z\alpha)^5}{\pi^2 n^3}\left(m_r^3 m\right)\int \frac{dq}{q^2}\, I(q^2)\left[G_E^2 - 1\right], \quad (30)$$

where

$$I(q^2) = \int_0^1 dv \frac{v^2(1 - v^2/3)}{4m^2 + (1 - v^2)q^2}. \quad (31)$$

The analytic presentation of $I(q^2)$ in a closed form is known as (cf., e.g., [49])

$$I(q^2) = \frac{\sqrt{q^2+4m^2}}{q^3}\left[\frac{1}{2}\ln\frac{\sqrt{q^2+4m^2}+q}{\sqrt{q^2+4m^2}-q} - \frac{q}{\sqrt{q^2+4m^2}}\right] - \frac{1}{3}\frac{(q^2+4m^2)^{3/2}}{q^5}\left[\frac{1}{2}\ln\frac{\sqrt{q^2+4m^2}+q}{\sqrt{q^2+4m^2}-q} - \frac{q}{\sqrt{q^2+4m^2}} - \frac{1}{3}\frac{q^3}{(q^2+4m^2)^{3/2}}\right], \quad (32)$$

which allows us to immediately perform a q integration numerically. It may be useful to apply the asymptotics of this expression, which are well known. In particular, at $q \ll m$ the asymptotic behavior is of the form

$$I(q^2) \simeq \frac{1}{15m^2} - \frac{q^2}{140m^4} + \cdots, \quad (33)$$

while at $q \gg m$ there is a logarithmic enhancement

$$I(q^2) \simeq \frac{1}{q^2}\left(\frac{1}{3}\ln\frac{q^2}{m^2} - \frac{5}{9}\right) + \frac{2m^2}{q^4} + \cdots. \quad (34)$$

The final results depend on a dimensionless parameter mR_N. In the case of ordinary (electronic) atoms, $mR_N \ll 1$. To reach this limit, we expect that $q \sim m$ and we have to expand the form factor in qR_N as

$$[G_E(q^2)]^2 - 1 \to 2[G_E(q^2) - 1] \simeq 2\left(-\tfrac{1}{6}R_N^2 q^2\right). \quad (35)$$

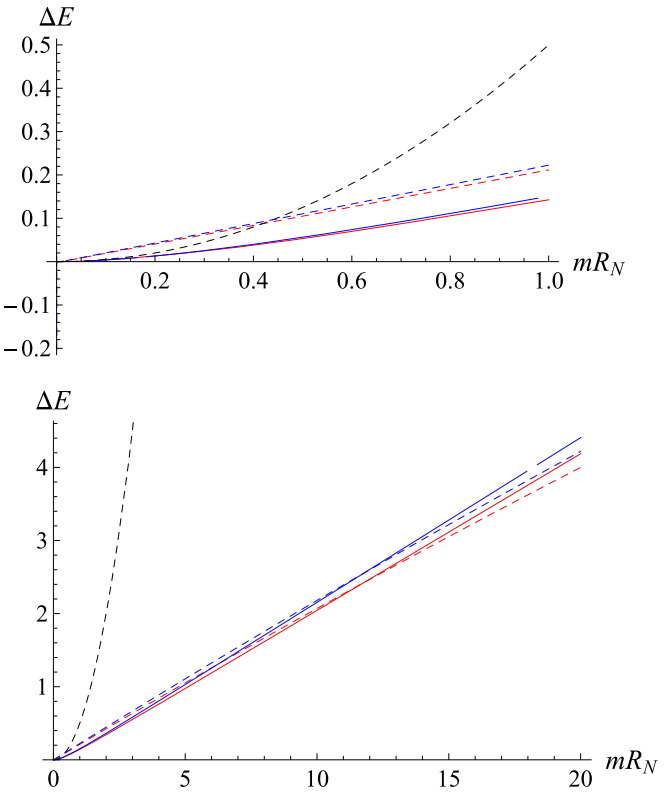

FIG. 8. The vacuum-polarization (VP) contribution to the ns Lamb shift in light muonic atoms in units of $\alpha(Z\alpha)^5 m_r^3/m^2/n^3$. The results are presented for the dipole parametrization and homogeneous-sphere distribution as a function of mR_N. The parameter for muonic hydrogen is $mR_N \simeq 0.43$. The colored dashed lines are for asymptotics at $mR_N \gg 1$, while the solid ones are for the direct calculations. The red and blue lines are for the dipole parametrization and the homogeneous-sphere distribution, respectively. The black dashed curve is for the ordinary-atom limit $mR_N \ll 1$ [see (37)], which is model-independent.

Once we use that expansion, starting with general expression (30), we arrive at the integral

$$\frac{16m}{\pi^2}\int_0^\infty dq\, I(q) = \frac{3}{4}. \tag{36}$$

The integrand depends on m as the dimensional scale parameter and therefore $q \sim m$, which validates the expansion in (35).

Further evaluation of the integral in (36) leads to the result that reads [50–52] (see [18] for more references and details)

$$\Delta E_{\text{fns:VP}}(ns) \simeq \tfrac{3}{4}\,\alpha(Z\alpha)\Delta E_{\text{fns:lead}}(ns). \tag{37}$$

In ordinary atoms such a limit (i.e., $mR_N \ll 1$) is perfectly appropriate, but not in the muonic ones. In [18] the result (together with the related SE FNS contribution) was suggested for use for muonic hydrogen. In muonic hydrogen $mR_N \simeq 0.43$, and as one can see from the plot in Fig. 8, the asymptotic formula in (37) is not really a good approximation. (The value of 0.43 relates to the standard dipole parametrization with $\Lambda^2 = 0.71\ \text{GeV}^2$. Use of the muonic-hydrogen value [1,14,53,54] leads to 0.45.)

Since the asymptotics at $mR_N \ll 1$ are not applicable for muonic hydrogen ($mR_N \simeq 0.43$), it might be interesting to consider the opposite asymptotic case at $mR_N \gg 1$. We do not expect it is an appropriate one for muonic hydrogen, but it might be, in principle, applicable for higher Z hydrogenlike muonic atoms.

Let us suppose that $q \sim R_N^{-1}$. Now one may expand the VP insertion in (31) at small q/m. Applying the first term of the asymptotics (33) at low q, we find

$$\Delta E_{\text{fns:VP}}(ns) \simeq -\frac{32\,\alpha(Z\alpha)^5}{15\pi^2 n^3}\frac{m_r^3}{m}\int\frac{dq}{q^2}\big[G_E^2 - 1\big]. \tag{38}$$

We note that the q integral is convergent and the characteristic value of q is $q \sim R_N^{-1}$, which makes appropriate the use of the low-q expansion.

The q-integral is merely the so-called first Zemach moment (similar to the one used for the hyperfine structure)

$$\begin{aligned}\langle r\rangle_{(2)} &\equiv \int d^3r \int d^3r'\,\rho(\mathbf{r})\,\rho(\mathbf{r}')\,|\mathbf{r}-\mathbf{r}'| \\ &= -\frac{4}{\pi}\int\frac{dq}{q^2}\big[G_E^2 - 1\big].\end{aligned} \tag{39}$$

Eventually, we arrive at

$$\Delta E_{\text{fns:VP}}(ns) \simeq \frac{8\alpha(Z\alpha)^5}{15\pi n^3}\frac{m_r^3}{m}\,\langle r\rangle_{(2)}. \tag{40}$$

Note that the two asymptotics [cf. (37) and (40)] have the same order in terms of α and $(Z\alpha)$. Namely, they are both of order $\alpha(Z\alpha)^5 m$. But they have a different order in terms of mR_N. While the former asymptotic is quadratic in this parameter, the latter is a linear one. If the latter limit would be saturated (for $mR_N \gg 1$), then they could differ by orders of magnitude. In light muonic atoms, we rather deal with a situation when the parameter is large but not very large [$mR_N \simeq 0.535(R_N/\text{fm})$]. Therefore, the difference between the asymptotics may not be too big. We have performed a straightforward evaluation of (30) and compared the asymptotic results and the result of the direct integration without any expansion (see Fig. 8). The evaluation is a model-dependent one, and in the plot of Fig. 8 we have considered the dipole parametrization and the homogeneous-sphere distribution of the charge. Many nuclear models are coordinate-space ones, and the presence of the asymptotics in (40) should facilitate calculations with such models.

V. CONTRIBUTIONS OF THE MUON SELF-ENERGY

A calculation of the SE FNS contribution is in many respects similar to the VP one (see the previous section). The related expression (see, e.g., [18]) has only one subtraction [cf. (30)]

$$\Delta E_{\text{fns:SE}}(ns) = -\frac{1}{2}\,\frac{32\alpha(Z\alpha)^5}{\pi^2 n^3}\,\frac{m_r^3}{m}\int\frac{dq}{q^2}[G_E^2 - 1]L(q), \tag{41}$$

where the lepton factor L is defined in [55,56]. A useful explicit presentation of the fermion-line factor is [57]

$$
\begin{aligned}
L(q) = &-\frac{1}{4}+\frac{1}{2}\ln\frac{q^2}{m^2}+\frac{1}{8}\frac{q^2}{m^2-q^2}\ln\frac{q^2}{m^2}\\
&-\frac{\sqrt{q^2+4m^2}}{2q}\ln\frac{\sqrt{q^2+4m^2}+q}{\sqrt{q^2+4m^2}-q}\\
&+\frac{m^2}{q\sqrt{q^2+4m^2}}\ln\frac{\sqrt{q^2+4m^2}+q}{\sqrt{q^2+4m^2}-q}\\
&-3\left[\frac{m^2}{q^2}-\frac{\sqrt{q^2+4m^2}\,m^2}{2q^3}\ln\frac{\sqrt{q^2+4m^2}+q}{\sqrt{q^2+4m^2}-q}\right]\\
&+\frac{q}{8m}\Phi(q)+\frac{m}{2q}\Phi(q)\\
&-\frac{2m^2}{q^2}\left[\frac{m}{q}\Phi(q)+\ln\frac{q^2}{m^2}-1\right],
\end{aligned}
\tag{42}
$$

where the function

$$
\Phi(q)=\int_0^1 dz\,\frac{mq}{m^2-q^2z^2}\ln\frac{m^2+q^2z(1-z)}{q^2z} \tag{43}
$$

can be expressed in terms of dilogarithms in a closed analytic form.

The asymptotic behavior of the lepton factor at low q ($q \ll m$) is (cf. [57])

$$
L(q)\simeq-\left(\frac{2}{3}\ln\frac{m^2}{q^2}+\frac{5}{9}\right)-\frac{q^2}{m^2}\left(\frac{7}{30}\ln\frac{m^2}{q^2}+\frac{67}{900}\right)+\cdots, \tag{44}
$$

while at $q \gg m$ the lepton factor becomes (cf. [57])

$$
\begin{aligned}
L(q)\simeq&-\frac{m^2}{q^2}\left(\frac{1}{3}\ln\frac{q^2}{m^2}+\frac{35}{36}\right)\\
&-\frac{m^4}{q^4}\left(\frac{41}{60}\ln\frac{q^2}{m^2}-\frac{167}{450}\right)+\cdots.
\end{aligned}
\tag{45}
$$

The latter is *not* for a "true" ultraviolet asymptotic limit. Such would be under condition $q, q_0 \gg m$ (where q_0 is the energy transfer) in the complete expression, while in the external field approximation the high-q asymptotics limit is for the situation with $q \gg m \gg q_0$. (That is, in the external field approximation we first set the energy transfer to zero, $q_0 = 0$, and next consider a large momentum transfer $|\mathbf{q}| \gg m$ for the high-q asymptotic limit.)

Similarly to the consideration in the previous section, we consider the asymptotics for the $\Delta E_{\rm fns:SE}(ns)$ at $mR_N \ll 1$ (the case of ordinary atoms) and at $mR_N \gg 1$ (the case of medium-Z muonic atoms).

To study the asymptotic behavior of the SE FNS contribution in (41) at the limit of the ordinary atoms ($mR_N \ll 1$), we apply the expansion of the form factor as in (35). After a simplification of the general expression (41), we find

$$
\frac{8}{\pi^2 m}\int_0^\infty dq\; L(q)=4\ln 2-\frac{23}{4}, \tag{46}
$$

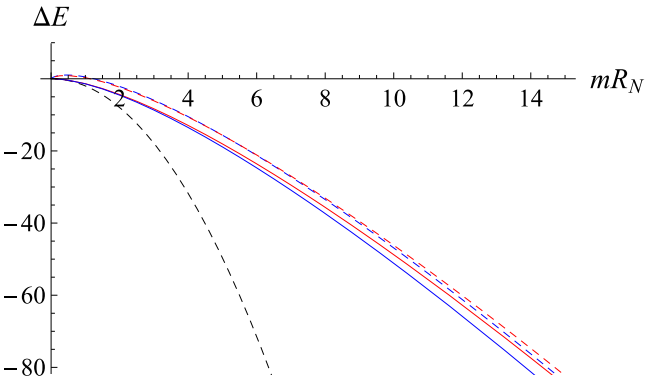

FIG. 9. The self-energy (SE) contribution to the ns Lamb shift in muonic atoms for various parametrizations as a function of mR_N (in muonic hydrogen $mR_N \simeq 0.43$). The units are $\alpha(Z\alpha)^5 m_r^3/m^2/n^3$. The dashed lines are for asymptotics, while the solid lines are for direct calculations. The red and blue lines are for the dipole parametrization and the homogeneous-sphere distribution. The black dashed curve is for the ordinary-atom limit ($mR_N \ll 1$), which is the same for both models. The colored asymptotics for $mR_N \gg 1$ are model-dependent.

which leads to the result [50–52] (see [18] for more references and details)

$$
\Delta E_{\rm fns:SE}(ns)=\left(4\ln 2-\frac{23}{4}\right)\alpha(Z\alpha)\Delta E_{\rm fns:lead}(ns). \tag{47}
$$

The opposite asymptotic case $mR_N \gg 1$, which corresponds to higher-Z muonic atoms, can be studied by using the low-q expansion of the lepton factor in (44). The result is

$$
\Delta E_{\rm fns:SE:as}(ns)=\frac{\alpha(Z\alpha)^5}{\pi n^3}\frac{m_r^3}{m}\left\langle r\left[\frac{2}{3}\ln\frac{1}{mr}+\frac{13}{18}-\frac{2}{3}\gamma\right]\right\rangle_{(2)}. \tag{48}
$$

The results of the direct calculation and the asymptotic ones are presented in Fig. 9. The estimations are performed with the dipole fit and with the homogeneous-sphere charge distribution.

Concluding the evaluation of the SE FNS contribution, let us mention a double-logarithmic term of higher order, namely of order $\alpha(Z\alpha)^6\ln^2(Z\alpha)m$. The correction is

$$
\Delta E(ns)=-\frac{8}{3}\frac{\alpha(Z\alpha)^2}{\pi}\ln^2 Z\alpha\left(\frac{m_r}{m}\right)^2\Delta E_{\rm fns:lead}(ns), \tag{49}
$$

which is found following the technique of [58,59] (see also [60]). That is an essentially nonrelativistic term and it is present both for ordinary and muonic atoms. The related diagram is depicted in Fig. 10.

Using a similar technique, one can also find a recoil double-logarithmic contribution of the order $(Z\alpha)^7(mR_N)^2m^2/M$ recoil contribution (cf. [58])

$$
\Delta E(ns)=-\frac{2}{3}\frac{(Z\alpha)^3}{\pi}\ln^2 Z\alpha\,\frac{m}{M}\left(\frac{m_r}{m}\right)^2\Delta E_{\rm fns:lead}(ns). \tag{50}
$$

However, it does not dominate numerically, since the $\ln(Z\alpha)$ term does not dominate (numerically) in the $(Z\alpha)^5m^2/M$ Salpeter term [61] in contrast to the standard leading term

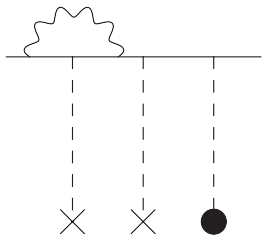

FIG. 10. A characteristic diagram for the higher-order double-logarithmic one-loop self-energy NFS term.

of order $\alpha(Z\alpha)^4 m$ (cf. [58]). It is essentially smaller than the nonrecoil double-logarithm in (49).

VI. NUMERICAL RESULTS

The equations, derived above for the eVP, VP, and SE FNS contributions in order $\alpha(Z\alpha)^5 m$ [see (16), (14), (21), (22), (30), and (41)], allow us to calculate the related contributions once we choose an appropriate presentation of the nuclear electric form factor or the nuclear charge density.

It may be interesting first to compare those four types of the radiative FNS contributions in order $\alpha(Z\alpha)^5 m$ considered above. The plot with all of them is presented in Fig. 11. For the model-dependent estimations, we use the homogeneous-sphere distribution.

To explain the relative behavior of the contributions, let us summarize here their asymptotic behavior and high Z and mR_N. In the leading logarithmic approximations, after setting $m_r = m$, the asymptotics take the simple form

$$\Delta E_{\text{fns:eVP:soft}}(ns) \simeq -\frac{4}{9}\,\frac{\alpha}{\pi}\,\frac{(Z\alpha)^5\,m}{n^3}\,\langle(mr)^3\rangle_{(2)}\,\ln\frac{Z\alpha m_\mu}{m_e},$$

$$\Delta E_{\text{fns:eVP:hard}}(ns) \simeq -\frac{4}{9}\,\frac{\alpha}{\pi}\,\frac{(Z\alpha)^5\,m}{n^3}\,\langle(mr)^3\rangle_{(2)}\,\ln\frac{1}{m_e R_N},$$

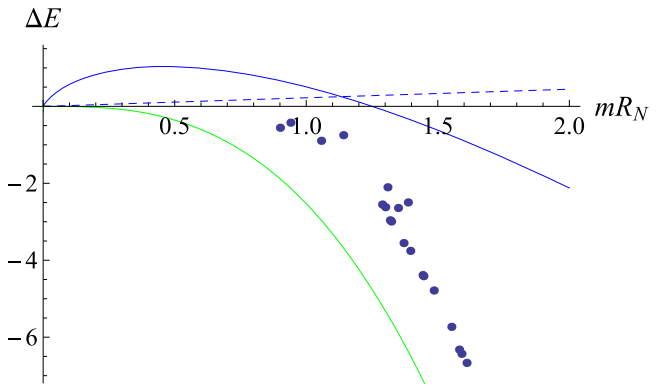

FIG. 11. Comparison of various radiative FNS contributions in order $\alpha(Z\alpha)^5 m$. The lines are for hard eVP (green), SE (blue solid), and (muonic) VP (blue dashed) contributions to the Lamb shift of the ns state as functions of mR_N. The eVP contributions are presented in units of $\alpha(Z\alpha)^5 m_r^4/m^3/n^3$, while the SE and VP ones are given in units $\alpha(Z\alpha)^5 m_r^3/m^2/n^3$. The difference in the units does not affect the plot too much. The closed circles are for the soft eVP contribution for the isotopes listed in Table I excluding hydrogen.

TABLE IV. Characteristic values of the nuclear-charge-radii parameters for the lightest muonic atoms. The parameters are given for two one-parameter parametrizations (see Appendix A for details); Λ is a parameter of the dipole parametrization and R is for the homogeneous-sphere distribution. The standard dipole model of the proton (with $\Lambda^2 = 0.71$ GeV^2) relates to $m_\mu R_N = 0.43$.

Nucleus	R_N (fm)	$m_\mu R_N$	Λ (GeV) (dipole)	R (fm)
deuteron	2.1	1.1	0.32	2.7
triton	1.7	0.91	0.40	2.2
helion	2.0	1.1	0.34	2.6
α particle	1.7	0.91	0.40	2.2

$$\Delta E_{\text{fns:VP}}(ns) \simeq \frac{8}{15}\,\frac{\alpha}{\pi}\,\frac{(Z\alpha)^5\,m}{n^3}\,\langle mr\rangle_{(2)},$$

$$\Delta E_{\text{fns:SE}}(ns) \simeq \frac{2}{3}\,\frac{\alpha}{\pi}\,\frac{(Z\alpha)^5\,m}{n^3}\,\langle mr\rangle_{(2)}\,\ln\frac{1}{mR_N}. \qquad (51)$$

The asymptotic results have different numeric coefficients, varying from 0.44 to 0.67, different scaling in mR_N (linear and cubic), and different logarithmic enhancements. For muonic hydrogen ($mR_N \simeq 0.43 < 1$), no logarithm, except for the one for the eVP:hard correction, is a big one. We have to combine all the radiative FNS contributions. For higher Z we note that both eVP contributions, which scale as $(mR_N)^3$, dominate over the SE and VP contributions, which scale as mR_N. Those two eVP contributions also have the biggest logarithmic enhancement.

To understand the location of the isotopes of muonic hydrogen and muonic helium ions in the plot, one has to look at Table IV. They relate to the area where the eVP contributions already dominate.

Because of the low value of mR_N and because of the high accuracy of the rest of the data, the Lamb shift in muonic hydrogen deserves separate consideration, and we start the discussion of the numerical result with it. The eVP contributions are corrections to the Friar term, the contribution of which is very uncertain by itself (see the discussion in [13,14,19]). The relation between the soft eVP FNS contribution and the Friar term has been considered above in a model-independent way [see (16) and (14)]. For the estimation of the hard eVP contribution, one may use the relation in (26). That is a relation between the hard eVP FNS contribution and the Friar term, obtained for the dipole parametrization. The electric form factor of the proton is relatively close to the dipole model, and we expect that the ratio of the hard eVP term and the Friar term deviates only weakly from the one for the dipole model. We estimate the deviation as less than 5%. Combining the hard and soft part, we find for the eVP FNS contribution to the Lamb shift in muonic hydrogen

$$\frac{\Delta E_{\text{fns:eVP}}(ns)}{\Delta E_{\text{fns:Fr}}(ns)} = \frac{\alpha}{\pi}\left(\frac{4}{3}\,\ln\frac{1}{m_e R_N} + 1.34\right). \qquad (52)$$

The numerical value here is for illustration only. For a "real" calculation one has to apply the expression from (52) with appropriate treatment of the Friar term. The uncertainty of the factor in the right-hand part of the identity, estimated by us

TABLE V. The fits: the related values of the nuclear radii and of the radiative FNS correction to the Lamb shift in muonic hydrogen. Here, $\Delta E_{\rm as}(mR_N \ll 1)$ stands for the asymptotics of ΔE_t at the limit $mR_N \ll 1$ (see the text). For the details of the fits, see Appendix B.

Fit	R_N (fm)	$\Delta E_{\rm VP}(ns)$ $[\alpha(Z\alpha)^5 m_r^3/m^2/n^3]$	$\Delta E_{\rm SE}(ns)$ $[\alpha(Z\alpha)^5 m_r^3/m^2/n^3]$	$\Delta E_{\rm VP+SE}/\Delta E_{\rm as}(mR_N \ll 1)$
(A1)	0.81	0.04336	–0.3056	0.936
(B6)	0.90	0.04980	–0.3677	0.919
(B5)	0.90	0.04947	–0.3642	0.920
(B1)	0.86	0.04700	–0.3405	0.926
(B2)	0.88	0.04811	–0.3509	0.923
(B3)	0.87	0.04739	–0.3432	0.926
(B4)	0.88	0.04804	–0.3506	0.923

as 5%, is smaller than the uncertainty of the evaluation of the Friar term itself.

To obtain numerical estimations, we apply the result from [13] with the proton radius as 0.84 fm,

$$\Delta E_{\rm fns:eVP}(ns) = -\frac{0.001\,95}{n^3}\ \text{meV}.$$

To evaluate the other (VP and SE) $\alpha(Z\alpha)^5 m$ FNS contributions, we apply various "realistic" fits of the proton charge form factor (see Appendix B). Those are the same fits as we used previously, while studying the Friar [19] and recoil FNS [13] contributions of order $(Z\alpha)^5 m$. The collection of the fits applied starts with the standard dipole fit, a few Padé approximations starting with Kelly's fit [62], and two chain-fraction fits [63]. We consider only fits that cover the whole range of q^2; the fits have different asymptotics at low and high q. In particular, the value of the charge radius related to the fits can be found in Table V.

We estimate the final result through the spread of the individual ones in Table V (see Appendix B for detail) as

$$\Delta E_{\rm fns:SE+VP}(2p-2s) = 0.038(1)\frac{\alpha(Z\alpha)^5 m_r^3}{m^2} = 4.4(1)\times 10^{-4}\ \text{meV}. \quad (53)$$

(We consider there all the fits from Table V but the dipole one, which is given since it is often used as a "standard" normalization.)

We note that all the realistic fits listed in the table produce results well consistent with the asymptotics in (37) and (47) for $mR_N \ll 1$ (which are denoted below as $\Delta E_{\rm fns:SE+VP:asym}$),

$$\Delta E_{\rm fns:SE+VP}(2p-2s) = 0.92(1)\times \Delta E_{\rm fns:SE+VP:asym}(2p-2s).$$

That result is very close to the use of the asymptotics only, as was suggested in [18] and used later on in many compilations.

In the meantime, one should remember that there is no working fit, consistent with the muonic-hydrogen value of the proton radius [1,14,53,54]. The "realistic" result should have an enlarged uncertainty, or one has to use the same approach as in [13,14,19]. The latter would be too cumbersome for such a small correction, and we prefer to somewhat enlarge the uncertainty and use 0.9(1) rather than 0.92(1).

Now let us consider the Lamb shift in other light muonic atoms. As we already mentioned discussing the plot in Fig. 11, the results for the isotopes of the muonic hydrogen atom and the muonic helium ion are very different from those for muonic hydrogen. In particular, we mentioned for the former the dominance of the eVP FNS contributions over the SE and VP ones. We summarize the numerical results on light muonic atoms in Tables VI and VII. For the numerical estimations, we use the homogeneous-sphere distribution.

Another important difference between muonic hydrogen and other light muonic atoms is in the use of the asymptotic formulas for the SE and VP terms. In the case of muonic hydrogen, the asymptotics at $mR_N \ll 1$ is not perfect, but still applicable for rough estimations. Meanwhile for the muonic deuterium, tritium, and ions of muonic helium and other light

TABLE VI. The radiative FNS corrections to the Lamb shift in light muonic atoms in order $\alpha(Z\alpha)^5 m$: $\Delta E_L(2p-2s)$ in units of $\alpha(Z\alpha)^5 m_r^3/m^2/8$. The numerical results for muonic hydrogen are explained in the text. The uncertainty for muonic hydrogen is not given; it should follow the uncertainty of the Friar term. They are found for $R_p = 0.84$ fm. The estimations for other elements are obtained by using the homogeneous-sphere distribution. The uncertainty here is only the statistical uncertainty due the uncertainty of R_N from Table I.

Nucleus	Z	eVP:soft	eVP:hard	VP	SE	Total
^{1}H	1	0.0381	0.2202	−0.0483	0.3528	0.5629
^{2}H	1	0.71(1)	3.47(5)	−0.1795(8)	1.764(8)	5.77(5)
^{3}H	1	0.41(6)	2.0(3)	−0.139(7)	1.26(6)	3.6(6)
^{3}He	2	0.86(2)	2.85(7)	−0.162(1)	1.54(1)	5.09(7)
^{4}He	2	0.541(4)	1.83(1)	−0.1308(3)	1.167(3)	3.41(1)
^{6}Li	3	2.4(1)	6.2(3)	−0.231(3)	2.46(4)	10.9(3)
^{7}Li	3	2.1(1)	5.3(3)	−0.214(4)	2.23(3)	9.4(3)
^{9}Be	4	2.61(4)	5.81(8)	−0.223(1)	2.35(1)	10.54(9)
^{10}B	5	2.6(1)	5.2(3)	−0.213(4)	2.21(5)	9.8(4)
^{11}B	5	2.52(9)	5.1(2)	−0.210(3)	2.17(3)	9.6(2)
^{12}C	6	2.965(8)	5.51(1)	−0.2174(2)	2.275(2)	10.54(2)
^{13}C	6	2.94(2)	5.46(2)	−0.2164(3)	2.261(3)	10.4(3)
^{14}N	7	3.52(3)	6.09(5)	−0.2273(6)	2.414(7)	11.80(6)
^{15}N	7	3.73(3)	6.42(6)	−0.2327(7)	2.491(8)	12.41(7)
^{16}O	8	4.38(3)	7.09(4)	−0.2433(5)	2.644(5)	13.87(5)
^{17}O	8	4.36(4)	7.05(6)	−0.2426(7)	2.634(7)	13.80(7)
^{18}O	8	4.76(3)	7.65(5)	−0.2517(5)	2.766(6)	14.9(5)
^{19}F	9	5.70(1)	8.66(2)	−0.2660(2)	2.979(3)	17.07(3)
^{20}Ne	10	6.63(1)	9.60(2)	−0.2783(2)	3.167(2)	19.12(2)
^{21}Ne	10	6.40(2)	9.28(3)	−0.2742(3)	3.104(3)	18.51(4)
^{22}Ne	10	6.29(3)	9.14(4)	−0.2722(4)	3.074(4)	18.23(5)

TABLE VII. The radiative FNS corrections to the Lamb shift in light muonic atoms in order $\alpha(Z\alpha)^5 m$: $\Delta E_L(2p-2s)$ in units of $10^{-3} E_{\text{lead:fns}}(2s)$ [see (1)]. The numerical results for muonic hydrogen are explained in the text. The muonic-hydrogen results are found for $R_p = 0.84$ fm. The uncertainty for the muonic hydrogen is not given; it should follow the uncertainty of the Friar term. The estimations for other elements are obtained by using the homogeneous-sphere distribution. The uncertainty here is only the statistical uncertainty due the uncertainty of R_N from Table I.

Nucleus	Z	eVP:soft	eVP:hard	VP	SE	Total
^{1}H	1	0.0150	0.0870	−0.0191	0.1393	0.2222
^{2}H	1	0.0436(6)	0.213(3)	−0.01102(5)	0.1083(5)	0.354(3)
^{3}H	1	0.037(5)	0.19(3)	−0.0125(6)	0.114(6)	0.32(3)
^{3}He	2	0.123(3)	0.41(1)	−0.0232(2)	0.221(2)	0.73(1)
^{4}He	2	0.107(8)	0.361(3)	−0.02578(6)	0.2301(5)	0.672(3)
^{6}Li	3	0.31(1)	0.78(4)	−0.0288(4)	0.307(5)	1.36(4)
^{7}Li	3	0.29(1)	0.74(4)	−0.0300(5)	0.313(5)	1.32(4)
^{9}Be	4	0.458(7)	1.02(1)	−0.0391(2)	0.413(2)	1.85(2)
^{10}B	5	0.61(4)	1.24(8)	−0.050(1)	0.52(1)	2.32(9)
^{11}B	5	0.61(2)	1.23(4)	−0.0506(6)	0.523(6)	2.31(5)
^{12}C	6	0.812(2)	1.510(4)	−0.05956(5)	0.6232(6)	2.886(5)
^{13}C	6	0.810(3)	1.507(6)	−0.05971(8)	0.6238(9)	2.881(7)
^{14}N	7	1.050(9)	1.82(1)	−0.0677(2)	0.719(2)	3.52(2)
^{15}N	7	1.07(1)	1.84(2)	−0.0668(2)	0.715(2)	3.56(2)
^{16}O	8	1.341(8)	2.17(1)	−0.0744(1)	0.809(2)	4.24(1)
^{17}O	8	1.34(1)	2.17(2)	−0.0746(2)	0.809(2)	4.24(2)
^{18}O	8	1.379(8)	2.22(1)	−0.0730(1)	0.802(2)	4.33(2)
^{19}F	9	1.701(4)	2.586(7)	−0.07943(7)	0.8897(8)	5.098(8)
^{20}Ne	10	2.045(4)	2.960(6)	−0.08584(6)	0.9769(7)	5.896(8)
^{21}Ne	10	2.021(7)	2.93(1)	−0.0866(1)	0.981(1)	5.85(1)
^{22}Ne	10	2.010(8)	2.92(1)	−0.0870(1)	0.983(1)	5.83(1)

muonic atoms, we note that the other asymptotics ($mR_N \gg 1$) are better (see Table IV for the related values of mR_N in light muonic atoms). The difference between the exact result and the asymptotic ones is between 20% and 25%, as one can see from Table VIII, which is sufficient for various rough estimations.

Table VII can also be used for Lyman transitions, data on which have been utilized for the determination of the nuclear charge radii for some elements (see the compilation [6] for details). Both the standard Lamb shift and the Lyman transitions deal with one s state (which is $2s$ for the Lamb shift measurement and $1s$ for a Lyman transition) and one p state. The results for the leading FNS term and the results for the $\alpha(Z\alpha)^5 m$ FNS contributions are determined by the s state since both the leading FNS contribution and the $\alpha(Z\alpha)^5 m$ one vanish for the p states. The ratio of the $\alpha(Z\alpha)^5 m$ FNS contribution to the leading FNS one does not depend on n and therefore the ratio has the same value for the np-$1s$ and $2p$-$2s$ intervals.

VII. CONCLUSIONS

We have evaluated above the $\alpha(Z\alpha)^5 m$ FNS contributions to the Lamb shift in light hydrogenlike atoms. The result consists of four terms: a soft eVP contribution (see Fig. 4), a hard eVP one (see Fig. 5), and [μ] VP (see Fig. 6) and SE (see Fig. 7) terms. We present numerical results as well as working formulas in coordinate and momentum space. The numerical results are presented up to $Z = 10$.

TABLE VIII. The radiative correction to the Lamb shift for the homogeneous-sphere distribution. The results are presented here without taking the statistical uncertainty due to the uncertainty in R_N into account. We apply here only the related central values from Table I.

Nucleus	$\Delta E_{\text{VP}}(ns)$ $[\alpha(Z\alpha)^5 m_r^3/m^2/n^3]$	$\Delta E_{\text{SE}}(ns)$ $[\alpha(Z\alpha)^5 m_r^3/m^2/n^3]$	$\Delta E_t/\Delta E_{\text{as}}$ $(mR_N \ll 1)$
^{2}H	0.1795	–1.7641	0.820
^{3}H	0.1386	–1.2587	0.854
^{3}He	0.1622	–1.5448	0.834
^{4}He	0.1308	–1.1668	0.861
^{6}Li	0.2308	–2.4639	0.783
^{7}Li	0.2145	–2.2338	0.794
^{9}Be	0.2229	–2.3518	0.788
^{10}B	0.2127	–2.2089	0.795
^{11}B	0.2102	–2.1749	0.797
^{12}C	0.2174	–2.2748	0.792
^{13}C	0.2164	–2.2610	0.793
^{14}N	0.2273	–2.4143	0.785
^{15}N	0.2327	–2.4910	0.781
^{16}O	0.2433	–2.6438	0.774
^{17}O	0.2426	–2.6340	0.774
^{18}O	0.2517	–2.7663	0.768
^{19}F	0.2660	–2.9791	0.759
^{20}Ne	0.2783	–3.1671	0.751
^{21}Ne	0.2742	–3.1040	0.754
^{22}Ne	0.2722	–3.0743	0.755

Some of those contributions have been studied previously. Speaking specifically about the FNS contributions to the Lamb shift in muonic hydrogen, we note that the whole eVP correction in order $\alpha(Z\alpha)^5 m$ is missing in the literature (see, e.g., [14,18,64]). In those publications, only VP and SE contributions have been considered. A similar situation exists with other radiative nuclear-structure corrections. For example, the whole eVP FNS correction is missing in order $\alpha(Z\alpha)^5 m$ for the muonic-hydrogen hyperfine splitting (see, e.g., [65]). The soft part of the eVP corrections to the nuclear polarizability contribution to the Lamb shift in muonic hydrogen is also missing in [66].

Calculation of the VP and SE $\alpha(Z\alpha)^5 m$ FNS contributions to the Lamb shift in muonic hydrogen have been considered in [18,64]. In [18], the SE and VP contributions have been suggested with the use of the asymptotic results in the limit $mR_N \ll 1$. That is a reasonable approximation for muonic hydrogen. For other elements with larger radii, such as, e.g., muonic deuterium, such an approximation is not adequate (see the previous section). In [64], the results for these two contributions have been obtained for muonic hydrogen and deuterium, and for both isotopes of muonic helium. The result is obtained with use of a dipole approximation with the actual values of the rms charge radius. We confirm those numerical results on muonic hydrogen and helium, but disagree for muonic deuterium. However, we have to mention that the dipole parametrization is not a good approximation for the nuclei of those muonic atoms. For muonic hydrogen we use

here realistic fits and study scatter of the related results, while for other mentioned atoms we use a homogeneous-sphere distribution.

To facilitate and simplify our consideration of the numerical results for light muonic atoms, we use two different one-parameter fits. One is the dipole parametrization and the other is the homogeneous-sphere distribution (see Appendix A). In such a case, a single parameter determines the charge radius of and the values of various contributions to the Lamb shift. We have plotted above the energy correction as a function of the value of the rms charge radius in Figs. 8 and 9. The fits utilized there are the dipole fit (A1) with a free parameter Λ and the homogeneous-sphere distribution [see (A3) and (A4)]. We do not consider the dipole fit as a realistic one and use it only to compare the asymptotic results and the direct ones.

In our final numerical estimations, we use "realistic" fits for muonic hydrogen (see the previous section) and the homogeneous-sphere distribution for the other light atoms. We do not pretend that the latter is a perfect approximation. However, it is good for estimations, and if more accurate calculations are needed one can perform them using an exact formula in momentum space or approximate ones in coordinate space, derived in this paper. Comparing the results for the dipole parametrization and the homogeneous-sphere distribution, we note that the deviation of the approximate asymptotic formulas from the exact ones does not depend much on the details of the charge distribution. Therefore, the deviation of the charge distribution from the homogeneous-sphere model can be found with the approximate formulas in coordinate space, while the contribution within the homogeneous-sphere model can be found with the exact equations in momentum space. Such a combination allows one a calculation for a broad class of the shapes of the nuclear charge distribution.

In the case of light muonic atoms, other than muonic hydrogen, the dominant contribution comes from eVP effects (see Fig. 11). For the calculation of the eVP FNS contributions, one can use formulas in momentum or coordinate space derived above in Sec. III. Since the asymptotic formulas for the VP and SE contributions at $mR_N \gg 1$ are more or less good for light muonic atoms, and since the related contributions are subdominant for all the atoms except for muonic hydrogen, the use of the asymptotic formulas in coordinate space seems sufficient.

One can apply our evaluations in two ways. To test QED one has to take certain values of the nuclear charge radii from "outside." The higher-order FNS effects are necessary for the tests with muonic atoms, and one has to consider the numerical values of various FNS contributions to the energy levels. Another possibility is to use QED theory and experimental data to determine the related nuclear charge radii. In this case the higher-order FNS effects should be presented as a function of the nuclear charge radius. That is most often possible only within a model. Many nuclear models deal with the charge density in coordinate space. The working formulas in coordinate space are derived above for all radiative FNS contributions in order $\alpha(Z\alpha)^5 m$ for light muonic atoms, other than muonic hydrogen.

We use above the one-parameter fits for rough plausible estimations. With every observable being expressed in terms of a single parameter, they introduce unphysical correlations between different physical nuclear observables, which are often not present in reality. In an actual situation, with the nuclear shape unknown, correlations come from sum rules (if any take place) and models. The models are used if we are missing accurate direct data. The availability of experimental data on various observables weakens the "theoretical" correlations. The experimental data are mostly available in momentum space for which we give expressions essentially simpler than have been available previously (cf. [64]).

Concluding, we present in this paper the numerical results, which are partly model-dependent, and the working expressions for the radiative FNS contributions of order $\alpha(Z\alpha)^5 m$ to the Lamb shift in light muonic atoms. The expressions are given both in coordinate and momentum space. The momentum-space expressions may be used when the experimental scattering data deliver a presentation of the electric form factor, while the coordinate-space ones are good for various nuclear models.

ACKNOWLEDGMENTS

The work related to the Lamb shift in muonic hydrogen was supported in part by DFG (under Grant No. KA 4645/1-1). The work on the other light muonic atoms was in part supported by RSF (under Grant No. 17-12-01036).

APPENDIX A: ONE-PARAMETER FITS APPLIED IN THE PAPER FOR LIGHT MUONIC ATOMS

To evaluate the Lamb shift in light muonic atoms in Sec. VI we use two one-parameter fits with the actual values of the nuclear charge radii (see Table I). Namely, we apply the dipole parametrization for the electric form factor and the homogeneous-sphere charge distribution. (We neglect the recoil effect and consider here the Fourier transform of the form factor as the distribution of the charge density.)

The dipole fit for the electric form factor

$$G_{\rm dip}(q^2) = \left(\frac{\Lambda^2}{q^2+\Lambda^2}\right)^2 \tag{A1}$$

is related to the exponential charge distribution

$$\rho_E(r) = \frac{\Lambda^3}{8\pi} e^{-\Lambda r}. \tag{A2}$$

The homogeneous-sphere charge distribution

$$\rho_E(\mathbf{r}) = \frac{3}{4\pi R^3}\Theta(R-|\mathbf{r}|) \tag{A3}$$

relates to the form factor

$$G_E(q) = \frac{3}{(qR)^2}\left[-\cos(qR) + \frac{\sin(qR)}{qR}\right]. \tag{A4}$$

Some parameters of those two fits are summarized in Table IX.

APPENDIX B: FITS FOR THE ELECTRIC FORM FACTOR OF THE PROTON APPLIED IN THE PAPER

We use in Sec. VI the following fits for the electric form factor of the proton for the calculation of the Lamb shift in

TABLE IX. Some geometrical properties of the one-parameter fits.

Fit	R_N	$\langle r\rangle_{(2)}/R_N$	$\langle r^3\rangle_{(2)}/R_N^3$
dipole (A1)	$\sqrt{12}/\Lambda$	$35/48\sqrt{3} \simeq 1.26$	$35/16\sqrt{3} \simeq 3.79$
homogeneous (A3)	$\sqrt{3/5}\,R$	$12/7\sqrt{3/5} \simeq 1.33$	$160/63\sqrt{5/3} \simeq 3.28$

muonic hydrogen: we apply a standard dipole parametrization (A1) with $\Lambda^2 = 0.71$ GeV^2 and utilize a few of Padé approximations starting with the simplest Kelly's fit [62]

$$G_E = \frac{1 - 0.24\tau_p}{1 + 10.98\tau_p + 12.82\tau_p^2 + 0.863\tau_p^3} \tag{B1}$$

through [67]

$$G_E = \frac{1 + 3.439\tau_p - 1.602\tau_p^2 + 0.068\tau_p^3}{1 + 15.055\tau_p + 48.061\tau_p^2 + 99.304\tau_p^3 + 0.012\tau_p^4 + 8.650\tau_p^5} \tag{B2}$$

and [68]

$$G_E(q^2) = \frac{1 - 0.19\tau_p}{1 + 11.12\tau_p + 15.16\tau_p^2 + 21.25\tau_p^3} \tag{B3}$$

to the most recent [69]

$$G_E(q^2) = \frac{1 + 2.909\,66\tau_p - 1.115\,422\,29\tau_p^2 + 3.866\,171 \times 10^{-2}\tau_p^3}{1 + 14.518\,7212\tau_p + 40.883\,33\tau_p^2 + 99.999\,998\tau_p^3 + 4.579 \times 10^{-5}\tau_p^4 + 10.358\,0447\tau_p^5}. \tag{B4}$$

We utilize also two chain-fraction fits [63]

$$G_E(q^2) = \cfrac{1}{1 + \cfrac{3.44Q^2}{1 - \cfrac{0.178Q^2}{1 - \cfrac{1.212Q^2}{1 + \cfrac{1.176Q^2}{1 - 0.284Q^2}}}}} \tag{B5}$$

and [63,70]

$$G_E(q^2) = \cfrac{1}{1 + \cfrac{3.478Q^2}{1 - \cfrac{0.140Q^2}{1 - \cfrac{1.311Q^2}{1 + \cfrac{1.128Q^2}{1 - 0.233Q^2}}}}}. \tag{B6}$$

Here Q is the numerical value for the momentum transfer q in GeV and $\tau_p = q^2/4m_p^2$.

A chain fraction is indeed also a Padé approximation. However, while the "standard" "Padé" fits (see above) are obtained suggesting asymptotic behavior q^{-4} at high momentum transfer, the chain-fraction fits have another high-q behavior, namely $\propto q^{-2}$. Use of the fits with different behavior at high q in the area, where no accurate experimental data are available, allows us to check whether the numerical results, obtained with those fits, depend on suggestions on the behavior of the fits at high q.

[1] P. J. Mohr, D. B. Newell, and B. N. Taylor, Rev. Mod. Phys. **88**, 035009 (2016).

[2] W. J. Huang, G. Audi, Meng Wang, F. G. Kondev, S. Naimi, and Xing Xu, Chin. Phys. C **41**, 030002 (2017); M. Wang, G. Audi, F. G. Kondev, W. J. Huang, S. Naimi, and Xing Xu, *ibid.* **41**, 030003 (2017).

[3] J. Arrington and I. Sick, J. Phys. Chem. Ref. Data **44**, 031204 (2015).

[4] I. Sick, Precise Radii of Light Nuclei from Electron Scattering, in *Precision Physics of Simple Atoms and Molecules*, edited by S. G. Karshenboim, Lecture Notes in Physics Vol. 745 (Springer, Berlin, 2007), pp. 57–77.

[5] I. Sick, J. Phys. Chem. Ref. Data **44**, 031213 (2015).

[6] I. Angeli and K. P. Marinova, At. Data Nucl. Data Tables **99**, 69 (2013).

[7] C. E. Carlson and M. Vanderhaeghen, Phys. Rev. A **84**, 020102(R) (2011).

[8] M. C. Birse and J. A. McGovern, Eur. Phys. J. A **48**, 120 (2012).

[9] A. A. Krutov, A. P. Martynenko, G. A. Martynenko, and R. N. Faustov, JETP **120**, 73 (2015).

[10] C. E. Carlson, M. Gorchtein, and M. Vanderhaeghen, Phys. Rev. A **89**, 022504 (2014).

[11] A. P. Martynenko and R. N. Faustov, Phys. At. Nucl. **67**, 457 (2004).

[12] C. E. Carlson, M. Gorchtein, and M. Vanderhaeghen, Phys. Rev. A **95**, 012506 (2017).

[13] S. G. Karshenboim, E. Yu. Korzinin, V. A. Shelyuto, and V. G. Ivanov, Phys. Rev. D **91**, 073003 (2015).

[14] S. G. Karshenboim, E. Yu. Korzinin, V. A. Shelyuto, and V. G. Ivanov, J. Phys. Chem. Ref. Data **44**, 031202 (2015).

[15] J. L. Friar, Ann. Phys. (N.Y.) **122**, 151 (1979).

[16] L. A. Borisoglebsky and E. E. Trofimenko, Phys. Lett. B **81**, 175 (1979).

[17] K. Pachucki, Phys. Rev. A **53**, 2092 (1996).

[18] M. I. Eides, H. Grotch, and V. A. Shelyuto, *Theory of Light Hydrogenic Bound States* (Springer, Berlin, 2007).

[19] S. G. Karshenboim, Phys. Rev. D **90**, 053012 (2014).

[20] S. G. Karshenboim, Phys. Lett. A **225**, 97 (1997).

[21] J. L. Friar and G. L. Payne, Phys. Rev. A **56**, 5173 (1997).

[22] J. L. Friar, Phys. Rev. C **88**, 034003 (2013).

[23] K. Pachucki, Phys. Rev. Lett. **106**, 193007 (2011).

[24] K. Pachucki and A. Wienczek, Phys. Rev. A **91**, 040503(R) (2015).

[25] C. Ji, N. Nevo Dinur, S. Bacca, and N. Barnea, Phys. Rev. Lett. **111**, 143402 (2013).

[26] O. J. Hernandez, C. Ji, S. Bacca, N. Nevo Dinur, and N. Barnea, Phys. Lett. B **736**, 344 (2014).

[27] N. Nevo Dinur, C. Ji, S. Bacca, and N. Barnea, Phys. Lett. B **755**, 380 (2016).

[28] O. J. Hernandez, N. Nevo Dinur, C. Ji, S. Bacca, and N. Barnea, Hyp. Int. **237**, 158 (2016).

[29] S. Weinberg, Phys. Lett. B **251**, 288 (1990); Nucl. Phys. B **363**, 3 (1991).

[30] D. R. Entem and R. Machleidt, Phys. Rev. C **66**, 014002 (2002).

[31] E. Epelbaum, W. Glockleb, and U.-G. Meissner, Nucl. Phys. A **747**, 362 (2005).

[32] D. R. Entem and R. Machleidt, Phys. Rev. C **68**, 041001 (2003).

[33] P. Navrátil, Few-Body Syst. **41**, 117 (2007).

[34] E. Epelbaum, H. Krebs, and U.-G. Meissner, Phys. Rev. Lett. **115**, 122301 (2015).

[35] H. Krebs, A. Gasparyan, and E. Epelbaum, Phys. Rev. C **85**, 054006 (2012); **87**, 054007 (2013).

[36] S. Binder, A. Calci, E. Epelbaum, R. J. Furnstahl, J. Golak, K. Hebeler, H. Kamada, H. Krebs, J. Langhammer, S. Liebig, P. Maris, U.-G. Meißner, D. Minossi, A. Nogga, H. Potter, R. Roth, R. Skibiński, K. Topolnicki, J. P. Vary, and H. Witała (LENPIC Collaboration), Phys. Rev. C **93**, 044002 (2016).

[37] J. L. Friar, Z. Phys. A **292**, 1 (1979); **303**, 84(E) (1981).

[38] E. Borie, Ann. Phys. **327**, 733 (2012).

[39] S. G. Karshenboim, V. G. Ivanov, and E. Yu. Korzinin, Phys. Rev. A **85**, 032509 (2012).

[40] S. G. Karshenboim, U. Jentschura, V. Ivanov, and G. Soff, Eur. Phys. J. D **2**, 209 (1998).

[41] S. G. Karshenboim, E. Yu. Korzinin, and V. G. Ivanov, JETP Lett. **88**, 641 (2008).

[42] D. Eiras and J. Soto, Phys. Lett. B **491**, 101 (2000).

[43] V. G. Ivanov, E. Yu. Korzinin, and S. G. Karshenboim, Phys. Rev. D **80**, 027702 (2009).

[44] A. P. Martynenko, Phys. Rev. A **71**, 022506 (2005).

[45] A. B. Mickelwait and H. C. Corben, Phys. Rev. **96**, 1145 (1954); G. E. Pustovalov, Sov. Phys. JETP **5**, 1234 (1957); D. D. Ivanenko and G. E. Pustovalov, Adv. Phys. Sci. **61**, 1943 (1957).

[46] S. G. Karshenboim, Can. J. Phys. **76**, 169 (1998); JETP **89**, 850 (1999).

[47] S. G. Karshenboim, V. G. Ivanov, and V. M. Shabaev, Can. J. Phys. **76**, 503 (1998); JETP **90**, 59 (2000).

[48] E. Borie, Phys. Rev. A **71**, 032508 (2005).

[49] L. D. Landau and E. M. Lifshitz, in *Course of Theoretical Physics*, edited by V. B. Berestetskii, E. M. Lifshitz, and L. P. Pitaevskii, Quantum Electrodynamics (Pergamon Press, Oxford, 1982), Vol. 4.

[50] K. Pachucki, Phys. Rev. A **48**, 120 (1993).

[51] M. I. Eides and H. Grotch, Phys. Rev. A **56**, R2507(R) (1997).

[52] A. I. Milstein, O. P. Sushkov, and I. S. Terekhov, Phys. Rev. Lett. **89**, 283003 (2002); Phys. Rev. A **67**, 062103 (2003).

[53] A. Antognini, F. Nez, K. Schuhmann, F. D. Amaro, F. Biraben, J. M. R. Cardoso, D. S. Covita, A. Dax, S. Dhawan, M. Diepold, L. M. P. Fernandes, A. Giesen, A. L. Gouvea, T. Graf, T. W. Hänsch, P. Indelicato, L. Julien, C.-Y. Kao, P. Knowles, F. Kottmann, E.-O. Le Bigot, Y.-W. Liu, J. A. M. Lopes, L. Ludhova, C. M. B. Monteiro, F. Mulhauser, T. Nebel, P. Rabinowitz, J. M. F. dos Santos, L. A. Schaller, C. Schwob, D. Taqqu, J. F. C. A. Veloso, J. Vogelsang, and R. Pohl, Science **339**, 417 (2013).

[54] R. Pohl, F. Nez, L. M. P. Fernandes, F. D. Amaro, F. Biraben, J. M. R. Cardoso, D. S. Covita, A. Dax, S. Dhawan, M. Diepold, A. Giesen, A. L. Gouvea, T. Graf, T. W. Hänsch, P. Indelicato, L. Julien, P. Knowles, F. Kottmann, E.-O. Le Bigot,Y.-W. Liu, J. A. M. Lopes, L. Ludhova, C. M. B. Monteiro, F. Mulhauser, T. Nebel, P. Rabinowitz, J. M. F. dos Santos, L. A. Schaller, K. Schuhmann, C. Schwob, D. Taqqu, J. F. C. A. Veloso, A. Antognini, and The CREMA Collaboration, Science **353**, 669 (2016).

[55] G. Bhatt H. Grotch, Ann. Phys. (N.Y.) **178**, 1 (1987).

[56] M. I. Eides and H. Grotch, Phys. Lett. B **301**, 127 (1993).

[57] M. I. Eides, H. Grotch, and V. A. Shelyuto, Phys. Rev. A **55**, 2447(R) (1997).

[58] S. G. Karshenboim, JETP **76**, 541 (1993).

[59] S. G. Karshenboim, JETP **82**, 403 (1996).

[60] S. G. Karshenboim and V. G. Ivanov, Phys. Rev. A **98**, 022522 (2018).

[61] E. E. Salpeter, Phys. Rev. **87**, 328 (1952).

[62] J. J. Kelly, Phys. Rev. C **70**, 068202 (2004).

[63] J. Arrington and I. Sick, Phys. Rev. C **76**, 035201 (2007).

[64] R. N. Faustov, A. P. Martynenko, F. A. Martynenko, and V. V. Sorokin, Phys. Lett. B **775**, 79 (2017).

[65] R. N. Faustov, A. P. Martynenko, G. A. Martynenko, and V. V. Sorokin, Phys. Lett. B **733**, 354 (2014).

[66] A. P. Martynenko and R. N. Faustov, Phys. At. Nucl. **64**, 1282 (2001).

[67] J. Arrington, W. Melnitchouk, and J. A. Tjon, Phys. Rev. C **76**, 035205 (2007).

[68] W. M. Alberico, S. M. Bilenky, C. Giunti, and K. M. Graczyk, Phys. Rev. C **79**, 065204 (2009).

[69] S. Venkat, J. Arrington, G. A. Miller, and X. Zhan, Phys. Rev. C **83**, 015203 (2011).

[70] P. G. Blunden, W. Melnitchouk, and J. A. Tjon, Phys. Rev. C **72**, 034612 (2005).